International Journal of Biomedical Science & Bioinformatics
Volume 3 : Issue 2 *[ISSN 2475 - 2290]*
Publication Date : 31 August, 2016

The Effect of Cu on Ni/γ-Al_2O_3 Catalyst for the Thermal Decomposition of Methane: An *ab initio* Molecular Dynamics Investigation

Gian Paolo O. Bernardo*, Leonila C. Abella, Joseph Auresenia, Hirofumi Hinode

***Abstract* — This study focuses on the catalytic decomposition of CH_4 for the production of carbon nanotubes (CNTs). The decomposition of a single CH_4 molecule on *Ni*/γ-Al_2O_3 catalyst surface with and without *Cu* was observed via *ab initio* calculations. The structural model was based on the transformation of metallic *Ni* and *Cu* into *Ni-Cu* alloy on γ-Al_2O_3 from experimental data. Structural relaxation and decomposition simulations were performed using Materials Studio 2016 DMol^3 with the Local Density Approximation – Vosko-Wilk-Nusair (LDA-VWM) exchange correlation functional, Gaussian double zeta plus polarization function basis set (DNP) at 2x2x1 k-point calculation and orbital cut-off of 3.5 Å, with simulation parameters: T = 1300K, time step = 1.9 fs (78.5 a.u.), simulation time of 0.38 ps, with canonical NVT (constant amount (N), volume (V) and temperature (T)) thermodynamic ensemble and Generalized Gaussian Moment (GGM) thermostat. Simulation data suggest lower *C* deposition at 1:1 *Ni-Cu.* Simulation data also suggest a weak *Ni* – γ-Al_2O_3 interaction characterized by the "lifting" of the *Ni* matrix and *Ni-Cu* alloy off of the γ-Al_2O_3 during CH_4 decomposition. The addition of *Cu* did not significantly alter the crystal size and structure of the *Ni*/γ-Al_2O_3 matrix. These results agree respectively with experimental findings: decreased CNT content with at 1:1 *Ni-Cu* content; CNT growth was found to follow the tip-growth model; and there was no significant correlation between the diameter of the CNT produced and *Cu* content in the catalyst. These findings demonstrate that the catalytic decomposition of CH_4 for the production of CNTs is environmentally promising via the modification of the metallic composition of the catalyst.**

Keywords*— *ab initio, alumina, carbon nanotubes, methane decomposition, molecular dynamics, nickel-copper

I. Introduction

The synthesis of carbon materials, such as carbon nanotubes (CNTs), has widely been done through Catalytic Chemical Vapor Deposition (CCVD) [1, 2] with *Ni*-based catalysts [3]. However, the susceptibility of Ni to carbon-deposition decreases catalytic activity due to the reduction of available active catalytic sites [4]. As such, various modifications have been done on *Ni*-based catalysts, to increase its catalytic performance and efficiency [5, 6].

One of the most common CCVD technologies is the Catalytic Thermal Decomposition of Methane (CTDM) [7] where, in line with the production of CNTs, *Ni-Cu*/γ-Al_2O_3 catalysts have been utilized due to the susceptibility of *Ni* and γ-Al_2O_3 to carbon deposition and the catalytic-promoting property of *Cu* [7, 8].

Molecular Dynamics (MD) simulations have been recently conducted on the mechanisms involving the dissociation and reaction of CH_4 on various catalytic surfaces [9-13], but so far only few have conducted simultaneous theoretical and experimental investigation on them.

In a previous work [13], the authors have investigated the decomposition of CH_4 on unsupported amorphous *Ni* and *Ni-Cu* purely through *Ab Initio* Molecular Dynamics (AIMD) simulation. In this study, similar AIMD investigations were conducted with the following key differences: layering of γ-Al_2O_3 support material underneath the *Ni* and *Ni-Cu* metal layers; the catalyst model was based on and compared with experimental data; and improvements on the AIMD simulation parameters.

Gian Paolo O. Bernardo
De La Salle University, Manila
Philippines

Leonila C. Abella; Joseph Auresenia
Chemical Engineering Department, Gokongwei College of Engineering, De La Salle University, Manila,
Philippines

Hirofumi Hinode
Department of International Development Engineering, Tokyo Institute of Technology, Tokyo,
Japan

SEEK DIGITAL LIBRARY

II. Design and Methodology

A. Model Parameters

The dissociation of a single CH_4 molecule on *Ni* and on *Ni-Cu* surfaces supported by γ-Al_2O_3 was investigated. The *Ni* surface was prepared from a single unit crystal of face-centered cubic (FCC) *Ni*, cleaved to (1 1 1) – associated with CH_4 dehydrogenation [14] – followed by structural relaxation.

The *Ni-Cu* surface was prepared by replacing symmetrically located *Ni* atoms into *Cu* atoms until the desired 1:1 *Ni:Cu* molar ratio was achieved, preserving the (1 1 1) configuration, followed by structural relaxation.

The support material was prepared from Hermann-Mauguin Fd-3m, Schoenflies group number 227 O7h or "213 P4132" Al_2O_3 corresponding to the lattice structure of γ-Al_2O_3 [15, 16], followed by structural relaxation.

The resulting metal layer was then mounted onto the γ-Al_2O_3 layer, preserving the lattice configuration of γ-Al_2O_3, followed by the final phase of structural relaxation.

A single CH_4 molecule was then added into the system. There were no physical constraints imposed on the system for system stability and to allow thermal expansion.

The resulting initial state structures are shown in Fig.1.

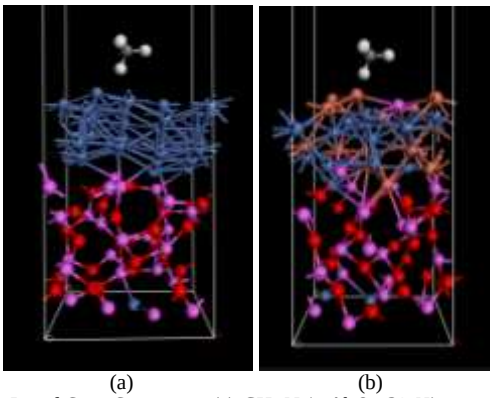

(a) (b)

Figure 1. Initial State Structures: (a) CH_4-Ni/γ-Al_2O_3: 32 *Ni* atoms, 85 total atoms; (b) CH_4-*Ni-Cu*/γ-Al_2O_3: 16 *Ni* atoms, 85 total atoms.

The atomic legend shown in Fig.2 applies to every other figure pertaining to the molecular model throughout this paper.

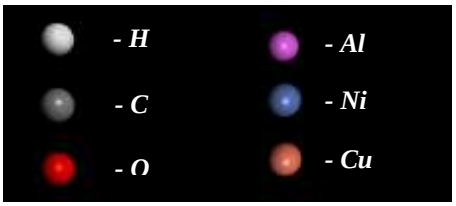

Figure 2. Atomic Legend

B. Computational Parameters

AIMD calculations were conducted through DMol^3 [17] with the Local Density Approximation (LDA) [17-20] the Vosko-Wilk-Nussair (VWN) [21] specific local exchange correlation functional and Gaussian double zeta plus polarization function (DNP) basis set [22]. The (2x2x1) k-point was used for Brillouin zone sampling with an orbital cut-off of 3.5 Å.

Dynamics simulations were conducted with a time step of 1.9 fs (78.5 a.u.) for a total simulation time of 0.38 ps (200 steps). The canonical NVT (constant amount (N), volume (V) and temperature (T)) thermodynamic ensemble [23] and Generalized Gaussian Moment [24] were used for temperature control at 1300K. The software environment and interface were contained in BIOVIA Accelrys Materials Studio 2016.

III. Results and Discussion

A. Crystal Size and Structure

The theoretical lattice parameters (lattice angles: α, β, γ; and cell volume) of the catalyst models are shown in Table 1.

TABLE I. CRYSTAL SIZE AND STRUCTURE DATA

Catalyst	Crystal Lattice Parameter			
	α	*β*	*γ*	*Cell Volume (Å^3)*
Ni/γ-Al_2O_3	90.1876°	89.4195°	89.5064°	1042.95
Ni-Cu/γ-Al_2O_3	89.9874°	90.0077°	89.89.16°	992.792

Calculations predict a 4.8% decrease in primitive (crystal) cell volume from *Ni/γ-Al_2O_3* to *Ni-Cu/γ-Al_2O_3*. This is counter-intuitive since *Cu* has a slightly larger atomic radius (128 pm, empirical) than *Ni* (124 pm, empirical). However, the difference in cell volume (4.8%) is still relatively similar to the difference in atomic radii (3.2%).

SEEK DIGITAL LIBRARY

This small change in crystal size is empirically supported by the independence of CNT diameter from *Cu* content in *Ni/γ-Al₂O₃*, determined through an on-going study by the authors.

Calculated X-Ray Diffractograms (XRD) for *Ni/γ-Al₂O₃* and *Ni-Cu/γ-Al₂O₃* are shown in Fig. 3 (a) and (b), respectively. The migration of the highest peak (▼) from 2θ = 46° (*Ni/γ-Al₂O₃*) to 2θ = 43.5° (*Ni-Cu/γ-Al₂O₃*) can be observed. This is in agreement with empirical characterization results by the authors shown in Fig.4.

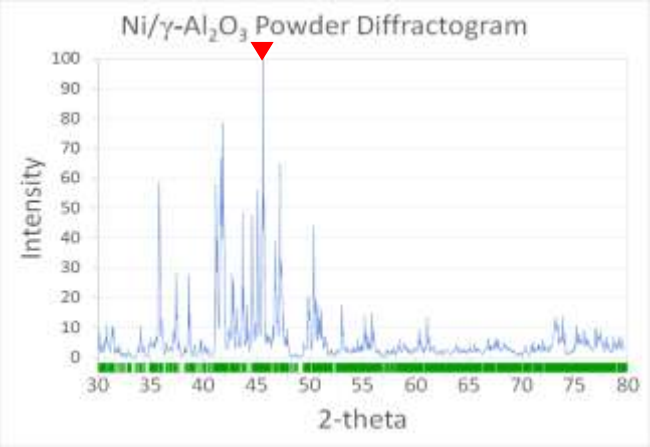

Figure 3a. Calculated Diffractogram for *Ni/γ-Al₂O₃*

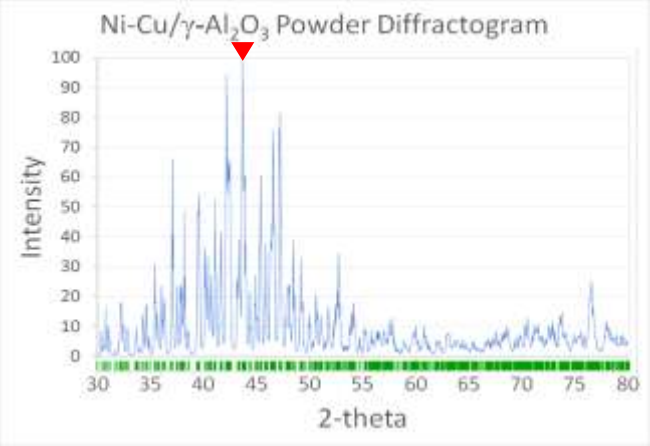

Figure 3b. Figure 3a. Calculated Diffractogram for *Ni-Cu/γ-Al₂O₃*

This peak migration can be attributed to the formation of a homogeneous *Ni-Cu* alloy – a determining factor in CNT production – while the difference between the empirical (2θ = 44°) and calculated (2θ = 46°) XRD angles can be attributed to the presence of more than one *Ni* crystal type (*Ni* (1 1 1), *Ni* (2 0 0) and *Ni* (2 2 0)).

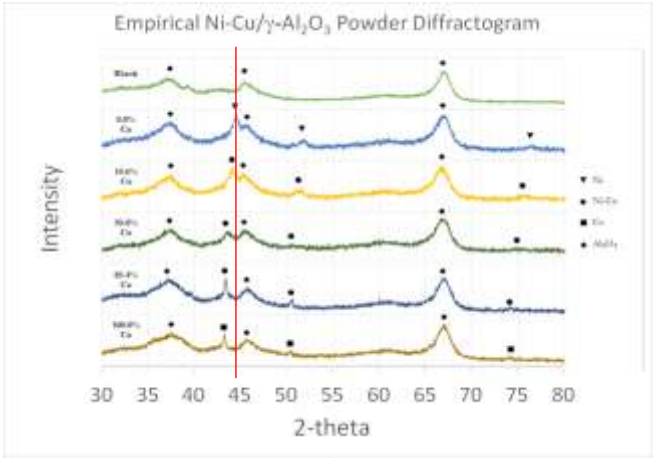

Figure 4. Empirical XRD Analysis for *Ni-Cu/γ-Al₂O₃* at varying *Ni-Cu* ratios

B. *Ab initio Molecular Dynamics*

Selected time course snapshots of the AIMD simulation of the decomposition of CH_4 on *Ni/γ-Al₂O₃* and on *Ni-Cu/γ-Al₂O₃* are shown in Fig. 5 and Fig. 6, respectively.

In the course of 51.3 fs, the number of bonds between *Ni* and *γ-Al₂O₃* has been dramatically reduced as a result of the upward trajectory, or "lifting", of the *Ni* layer from the *γ-Al₂O₃* layer. This suggests a weak interaction between the *Ni* layer from the *γ-Al₂O₃* layer.

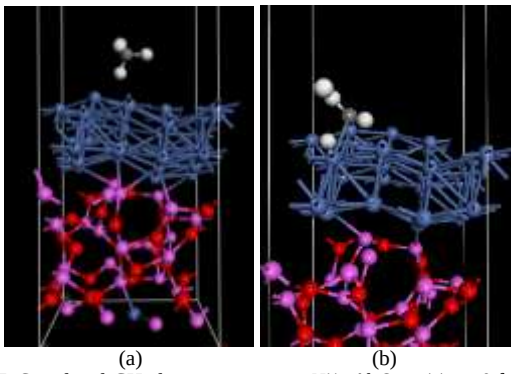

(a) (b)

Figure 5. Simulated CH_4 decomposition on *Ni/γ-Al₂O₃* at (a) t = 0 fs and (b) t = 51.3 fs

On the other hand, even at t = 68.4 fs, the number of bonds between the *Ni-Cu* layer and the *γ-Al₂O₃* layer has not decreased significantly. Consequently, the upward trajectory

SEEK DIGITAL LIBRARY

of the *Ni-Cu* layer is not as pronounced as the *Ni* layer trajectory.

C deposition has been predicted for both $Ni/\gamma\text{-}Al_2O_3$ and on $Ni\text{-}Cu/\gamma\text{-}Al_2O_3$, whereas the presence of *Cu* accelerated the annihilation of the CH_4 molecule into free *H* atoms and a depositing *C* atom, similar to a previous study [13].

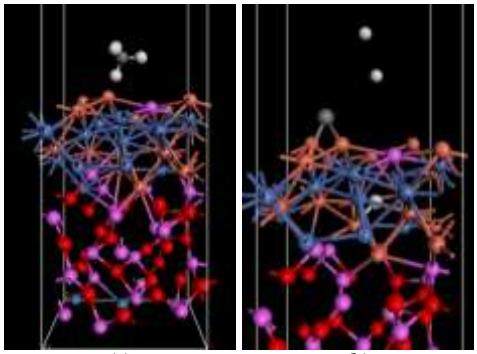

(a) (b)

Figure 6. Simulated CH_4 decomposition on $Ni\text{-}Cu/\gamma\text{-}Al_2O_3$ at (a) t = 0 fs and (b) t = 68.4 fs

Further into the simulation, at t > 83.6 fs, as shown in Fig. 7. The *C* deposition process on $Ni/\gamma\text{-}Al_2O_3$ is more persistent than that on $Ni\text{-}Cu/\gamma\text{-}Al_2O_3$ as demonstrated by the catenation of the *C-metal* bonds in Fig. 7b in comparison with the persistence of the *C-metal* bonds in Fig. 7a. This, in conjunction with the accelerated annihilation of the CH_4 molecule, confirms the catalytic promoting property of *Cu* by discouraging or limiting the *C*-deposition process at high (>50%) *Cu* content while enhancing the catalytic activity of *Ni*.

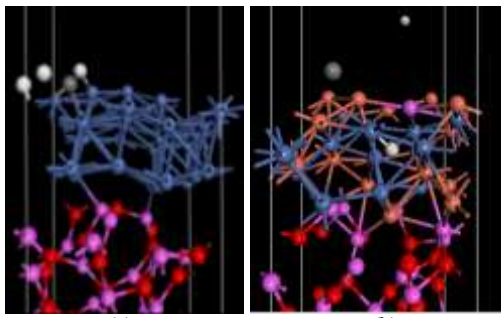

(a) (b)

Figure 7. Carbon deposition on (a) $Ni/\gamma\text{-}Al_2O_3$ and (b) $Ni\text{-}Cu/\gamma\text{-}Al_2O_3$

These calculations agree with empirical data from Scanning Electron Microscopy (SEM) (Fig. 8) and ThermoGravimetric Analysis (TGA) (Fig. 9) where more CNTs were produced on $Ni/\gamma\text{-}Al_2O_3$ than on $Ni\text{-}Cu/\gamma\text{-}Al_2O_3$. CNT nucleation was also observed to follow the tip-growth model as shown in Fig. 8, indicated by the presence of white metallic tips on the grown nanotubes, suggesting the same weak $Ni/\gamma\text{-}Al_2O_3$ interaction determined from AIMD.

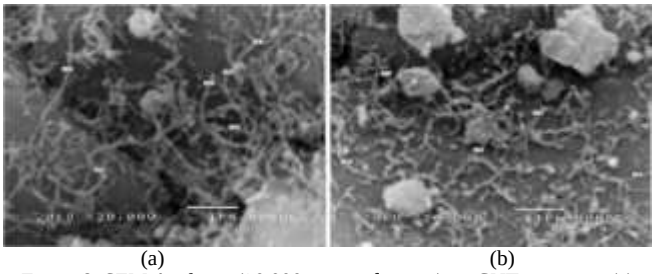

(a) (b)

Figure 8. SEM Analyses (20,000x magnification) on CNT grown on (a) $Ni/\gamma\text{-}Al_2O_3$ and (b) $Ni\text{-}Cu/\gamma\text{-}Al_2O_3$

In effect, the addition of *Cu* enhanced the interaction between the *Ni-Cu* layer and the $\gamma\text{-}Al_2O_3$ layer. This, in addition to the decrease in CNT yield as shown in Fig. 9, is in agreement with the decrease in the primitive cell volume with the addition of *Cu* on $Ni/\gamma\text{-}Al_2O_3$, whereas a stronger inter-cellular interaction results in a decrease in crystal size as a result of shorter average bond lengths.

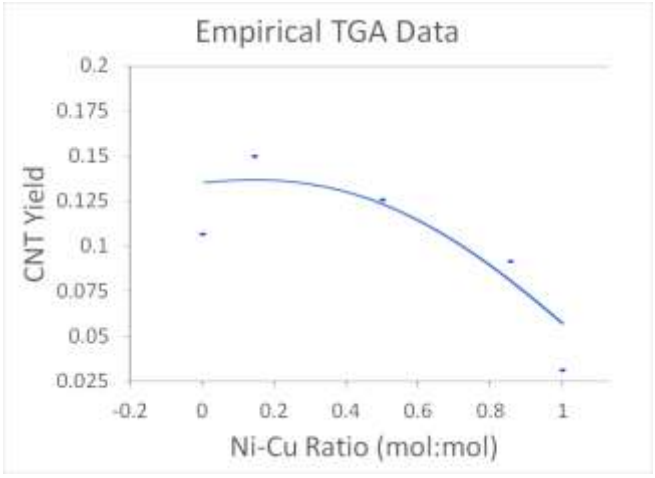

Figure 9. TGA for CNT Yield on experimentally-prepared $Ni/\gamma\text{-}Al_2O_3$ at varying *Cu* content after CTDM.

IV. Conclusions

The effect *Cu* promoter on $Ni/\gamma\text{-}Al_2O_3$ was successfully investigated through AIMD simulations with empirical concurrence. The addition of *Cu* enhanced the metal-support interaction resulting in a 4.8% decrease in the crystal size and the destabilization of the *C* deposition mechanism, further resulting to a predicted decrease in CNT production

SEEK DIGITAL LIBRARY

leading to the decrease in the initial *C* deposition rate and the suppression of the tip-growth mechanism. On the other hand, AIMD simulations on *Ni/γ-Al_2O_3* in the absence of *Cu* predict a weak metal-support interaction and a more stable *C* deposition mechanism, leading to increased CNT production via the tip-growth mechanism. These results suggest an optimum *Cu* content (0% < x 50%), the determination of which can be subject to further studies. Furthermore, this concurrence of simulation data with empirical data is significant to the production of CNTs from CTDM in the field of AIMD simulations, opening more specific and directed avenues for future research.

Acknowledgments

This research was made possible through the Engineering Research for the Development of Technology – Department of Science and Technology (ERDT-DOST) scholarship program, through De La Salle University – Manila in collaboration with the Tokyo Institute of Technology.

References

[1] Y.A.Zhu, D.Chen, X.G.Zhou, W.K.Yuan, "DFT studies of dry reforming of methane on Ni catalyst", Catalysis Today, 148, 260-267 (2009).

[2] E.Kurnaz, M.F.Fellah, I.Onal, "A density functional theory study of C-H bond activation of methane on a bridge site of M-O-M-ZSM-5 Clusters (M = Au, Ag, Fe and Cu)", Microsoporous and Mesoporous Materials, 138, 68-74 (2011).

[3] F.Pompeo, N.N.Nichio, M.M.V.M.Souza, D.V.Cesar, O.A.Ferretti, M.Schmal, "Study of Ni and Pt catalysts supported on a-Al_2O_3 and ZrO_2 applied in methane reforming with CO_2", Applied Catalysis A: General, 316, 175-183 (2007).

[4] V.V.Cheskonov, A.S.Chichkan, "Production of hydrogen by methane catalytic decomposition over Ni-Cu-Fe/Al_2O_3 catalyst", Hydrogen Energy, 34, 2979-2985 (2009).

[5] A.Romero, A.Garrido, A.Niteo-Márquez, A.R.de la Osa, A.de Lucas, J.L.Valverde, "The influence of operating conditions on the growth of carbon nanofibers on carbon nanofiber-supported nickel catalysts", Applied Catalysts A: General, 319, 246-258 (2007).

[6] J.Y.Gu, K.X.Li, J.Wang, H.W.He, "Control growth of carbon nanofibers on Ni/activated carbon in a fluidized bed reactor", Microporous and Mesoporous Materials, 131, 393-400 (2010).

[7] V.V.Cheskonov, A.S.Chichkan, "Production of hydrogen by methane catalytic decomposition over Ni-Cu-Fe/Al_2O_3 catalyst", Hydrogen Energy 34, 2979-2985 (2009).

[8] J .L. Pinilla, M. J. Lázaro, I. Suelves, R. Moliner, J. M. Palacios, "Characterization of nanofibrous carbon produced at pilot-scale in a fluidized bed reactor by methane decomposition", Chem. Eng., 156, 170-176 (2010).

[9] Y. Shibuta, R. Arifin, K. Shimamura, T. Oguri, F. Shimojo, S.Yamaguchi, "Ab initio molecular dynamics simulation of dissociation of methane on nickel(111) surface: Unravelling initial stage of graphene growth via a CVD technique", Chem. Phys. Letters 565, 92-97 (2013).

[10] K. Li, C. He, M. Jiao, Y. Wang, Z. Wu, "A first-principles study on the role of hydrogen in early stage graphene growth during the CH_4 dissociation on Cu(111) and Ni(111) surfaces", Carbon, 74, 255-265 (2014).

[11] W. Zhu, A. Börjesson, K. Bolton, "DFT and tight binding Monte Carlo calculations related to single-walled carbon nanotube nucleation and growth", Carbon, 48, 470-478 (2010).

[12] B. Liu, M. T. Lusk, J. F. Ely, "Reactive molecular dynamic simulations of hydrocarbon dissociations on Ni(111) surfaces", Surf. Sci., 606, 615-623 (2012).

[13] G.P.O.Bernardo, L.C.Abella, J.Auresenia, H.Hinode, "Effect of Cu on Ni Catalyst for the Thermal Decomposition of Methane: A Molecular Dynamics Investigation", Int. J. Chem. Eng., 2:1, 95-99 (2015).

[14] J. Li, E. Croiset, L. Ricardez-Sandoval, "Effect of carbon on the Ni catalyzed methane cracking reaction: A DFT study", App. Surf. Sci., 311, 435-442 (2014).

[15] X-ray powder diffraction file, JCPDS 50-741 (2002).

[16] X-ray powder diffraction file, JCPDS 10-425 (2002).

[17] B. Delley, "From Molecules to Solids with the DMol3 Approach", J. Chem. Phys, 113, 7756 (2000).

[18] L. Hedin, B. I. Lundqvist, "Explicit local exchange correlation potentials", Phys. C, 4, 2064-2083 (1971).

[19] D. M. Ceperley, B. J. Alder, "Ground state of the electron gas by a stochastic method", Phys. Rev. Lett., 45, 566-569 (1980).

[20] S. Lundqvist, N. March, Eds., Theory of the Inhomogeneous Electron Gas, Plenum: New York (1983).

[21] S. H. Vosko, L. Wilk, M. Nusair, "Accurate spin-dependent electron liquid correlation energies for local spin density calculations: a critical analysis", Can. J. Phys., 58, 1200-1211 (1980).

[22] B. J. Delley, "An all‐electron numerical method for solving the local density functional for polyatomic molecules", Chem. Phys., 92, 508 (1990).

[23] S. Nosé, "A molecular dynamics method for simulations in the canonical ensemble", Mol. Phys., 52, 255-268 (1984).

[24] M. E. Tuckerman, Y. Liu, "Generalized Gaussian moment thermostatting: a new continuous dynamical approach to the canonical ensemble", J. Chem. Phys., 112, 1685 (2000).

About the Author:

"This concurrence of simulation data with empirical data is significant to the production of CNTs from CTDM in the field of AIMD simulations, opening more specific and directed avenues for future research.

SEEK DIGITAL LIBRARY